Uranium-Series Constraints on Radionuclide Transport and Groundwater Flow at the Nopal I Uranium Deposit, Sierra Peña Blanca, Mexico

STEVEN J. GOLDSTEIN,*,† AMR I. ABDEL-FATTAH,‡ MICHAEL T. MURRELL,† PATRICK F. DOBSON,§ DEBORAH E. NORMAN,† RONALD S. AMATO,† AND ANDREW J. NUNN†

Nuclear and Radiochemistry Group, Los Alamos National Laboratory, P.O. Box 1663, MS J514, Los Alamos, New Mexico 87545, Earth and Environmental Sciences Division (EES-14), Los Alamos National Laboratory, P.O. Box 1663, MS J966, Los Alamos, New Mexico 87545, and Earth Sciences Division, Lawrence Berkeley National Laboratory, Berkeley, California 94720

Received September 4, 2009. Revised manuscript received January 13, 2010. Accepted January 13, 2010.

Uranium-series data for groundwater samples from the Nopal I uranium ore deposit were obtained to place constraints on radionuclide transport and hydrologic processes for a nuclear waste repository located in fractured, unsaturated volcanic tuff. Decreasing uranium concentrations for wells drilled in 2003 are consistent with a simple physical mixing model that indicates that groundwater velocities are low (~10 m/y). Uranium isotopic constraints, well productivities, and radon systematics also suggest limited groundwater mixing and slow flow in the saturated zone. Uranium isotopic systematics for seepage water collected in the mine adit show a spatial dependence which is consistent with longer water−rock interaction times and higher uranium dissolution inputs at the front adit where the deposit is located. Uranium-series disequilibria measurements for mostly unsaturated zone samples indicate that $^{230}Th/^{238}U$ activity ratios range from 0.005 to 0.48 and $^{226}Ra/^{238}U$ activity ratios range from 0.006 to 113. $^{239}Pu/^{238}U$ mass ratios for the saturated zone are $<2 \times 10^{-14}$, and Pu mobility in the saturated zone is >1000 times lower than the U mobility. Saturated zone mobility decreases in the order $^{238}U \approx {}^{226}Ra > {}^{230}Th \approx {}^{239}Pu$. Radium and thorium appear to have higher mobility in the unsaturated zone based on U-series data from fractures and seepage water near the deposit.

Introduction

Geological barriers are an important possible mechanism for isolation of radioactive contaminants from the biosphere. One measure of the effectiveness of such barriers is determination of retardation factors, i.e., the transport rate of contaminants relative to groundwater. Uranium-series techniques are an important method for determining in situ retardation factors in groundwater (e.g., *1*−*3*). In a geochemical system that is closed for greater than five daughter half-lives, the activity of each U-series daughter will be equivalent to that of its parent nuclide. This is true for rocks that have been closed systems for approximately one million years. However, as U-series nuclides are dissolved in groundwater during water−rock interaction, chemical fractionations may occur between different elements which result in disequilibria among U-series nuclides. For long-lived U-series daughters where decay in groundwater is negligible, the magnitude of U-series disequilibria is proportional to the relative mobility of each U-series nuclide in groundwater. As an approximation, the extent of U-series disequilibria is also inversely related to relative retardation factors. Hence, measurement of long-lived daughters such as ^{234}U, ^{230}Th, ^{226}Ra, and ^{239}Pu can be used to directly determine their relative mobility or retardation in groundwater.

We have applied these techniques to study groundwater flow and radionuclide transport near the Nopal I uranium deposit located in the Peña Blanca region, Chihuahua, Mexico (Figure 1). This area, approximately 50 km north of Chihuahua City, was a major target of uranium exploration and mining by the Mexican government in the 1970s. More recently, this deposit has been extensively studied as an analog for evaluating the fate of spent fuel, associated actinides, and fission products at a geologic repository in fractured, unsaturated volcanic tuff. Briefly, the deposit represents an environment similar to that of the proposed U.S. Yucca Mountain high-level radioactive waste repository in the following ways: (1) climatologically, both are located in semiarid to arid regions, (2) structurally, both are parts of a basin-and-range horst structure composed of Tertiary rhyolitic tuffs overlying carbonate rocks, (3) hydrologically, both are located in a chemically oxidizing environment within an unsaturated zone, 200 m or more above the water table, and have broadly similar water chemistries, and (4) chemically, because the alteration of primary uraninite (*4*) to secondary uranium minerals at Nopal I may be similar to the eventual fate of uranium fuel rods in a geologic repository according to results of spent-fuel alteration experiments (*5*). In this study, we measured long-lived U-series nuclide abundances in groundwater from this site by sensitive mass spectrometric methods. U-series measurements, including our measurements of $^{238}U-{}^{239}Pu$ disequilibrium, are used to constrain recent radionuclide transport and groundwater hydrologic processes at this location. This provides a unique opportunity to follow transport of U-series nuclides in three dimensions from a well-defined source term, namely the ore body. Our study may add to the conceptual understanding of similar processes at the proposed Yucca Mountain repository or other waste disposal sites in semiarid, unsaturated zone settings.

Samples and Methods

Saturated zone (SZ) waters were collected from 6 wells near the Nopal I uranium deposit, and seepage waters from the unsaturated zone (UZ) were obtained from an adit at the Nopal I mine (Figures 1 and 2). SZ intervals of the PB1, PB2, and PB3 wells, located immediately adjacent to the Nopal I ore deposit, occur mostly within Pozos conglomerate, with the lowest section of each well in Cretaceous limestone (*6*). SZ intervals for two wells located SE of the Nopal I deposit,

* Corresponding author e-mail: sgoldstein@lanl.gov; phone: 505-665-4793; fax: 505-665-4955.

† Nuclear and Radiochemistry Group, Los Alamos National Laboratory.

‡ Earth and Environmental Sciences Division (EES-14), Los Alamos National Laboratory.

§ Earth Sciences Division, Lawrence Berkeley National Laboratory.

10.1021/es902689e Not subject to U.S. Copyright. Publ. XXXX Am. Chem. Soc.

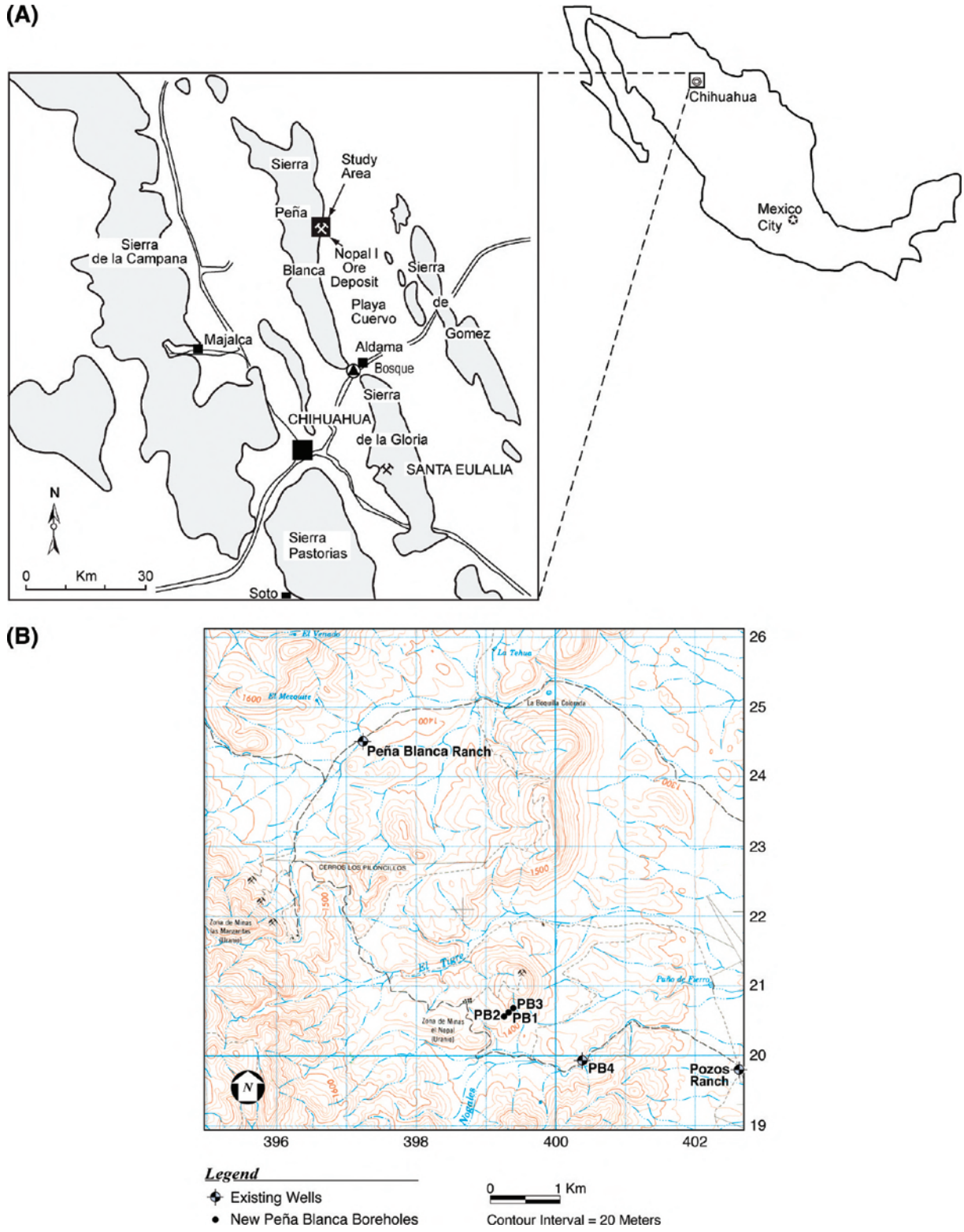

FIGURE 1. (A) General location of study area. Assumed direction of groundwater flow is from the west to the east from the Sierra Peña Blanca toward the Playa Cuervo. Bosque near Aldama is the location of sampling of the Chuviscar River by Villalba et al (*10*). (B) Location of wells in this study. Base map taken from Instituto de Estadística, Geografía e Informática 1:50,000 El Sauz topographic map (H13C46).

PB4 and Pozos Ranch, are totally within Cretaceous limestone. The subsurface geology at Peña Blanca Ranch is not constrained near the water table.

UZ water sample locations from the mine adit are shown in Figure 2. The mine adit is located at the +00 level of the deposit near PB1. UZ rocks near the mine adit consist of rhyolitic welded ash-flow tuffs (Nopal and Coloradas Formations) that host the ore deposit (*6*). Groundwater samples from the adit and regional wells were collected during 2000−2006, whereas samples from the PB1, PB2, and PB3 wells have been collected from 2003−2006.

SZ water samples were mostly collected by bailer, but in two instances (December 2003 and August 2006) they were collected by pump. UZ water samples were collected from

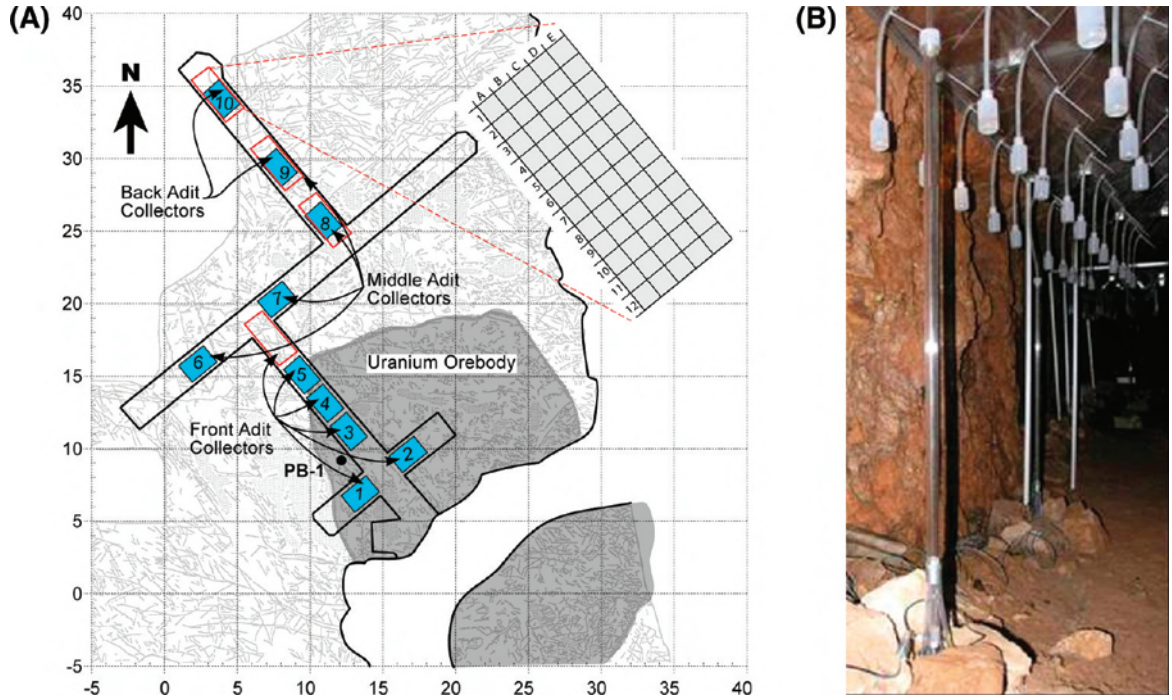

FIGURE 2. (A) Schematic map of the UACH (Universidad Autónoma de Chihuahua) and LBNL (Lawrence Berkeley National Laboratory) unsaturated zone sample collection sites from the mine adit located on the +00 level. The collectors consisted of plastic sheeting which was designed to funnel seepage water into plastic bottles (blue boxes; UACH), or a fine grid of hard plastic collectors and bottles (red outlined boxes; LBNL). The LBNL collectors replaced the UACH collectors in 2005. Locations of the UACH collectors are approximate only. (B) Photo of the array of LBNL seepage collectors along with a column equipped with transducers to measure the timing and volume of seepage events.

the mine adit via two collection systems (Figure 2): initially a drip collection system consisting of plastic sheeting and later a rigid plastic grid that was designed to funnel water into plastic bottles. Water samples for U-series analyses were filtered (0.20 or 0.45 μm filters) after collection and acidified to a pH of 1−2 with high-purity nitric acid for long-term storage. Samples from the PB1 and PB4 wells collected specifically for colloid analysis were stored in coolers immediately after collection and refrigerated until analysis. These samples were ultrafiltered in the laboratory using separate sterile ultrafiltration stirred cells (Millipore, USA), equipped with both 300 kDa (kilodalton) membrane filters and 20-nm in-line syringe filters. U concentrations of unfiltered and filtered splits were measured to determine how much of the U is associated with colloids.

Uranium, thorium, radium, and plutonium samples were analyzed as separate aliquots and each was spiked with ^{233}U, ^{229}Th, ^{228}Ra, or ^{244}Pu tracer. After tracer equilibration, uranium was purified using anion exchange columns and loaded onto single or triple Re filaments (*7*). Uranium isotopes (^{238}U, ^{235}U, ^{234}U) were measured multistatically using a GV Sector 54 mass spectrometer equipped with multiple Faraday cups and a Daly ion counting detector. Calibration between Daly and Faraday detectors was determined by switching the ^{235}U beam between these collectors, and instrumental mass fractionation was corrected by normalization to the natural ^{238}U/^{235}U ratio of 137.88.

Radium was purified using cation exchange columns for the major element separation, EDTA-cation columns for Ra−Ba separation, and a final cation exchange column to rid the samples of EDTA. Radium was loaded onto Pt filaments using a silica gel enhancer and analyzed dynamically on a NBS 12-90 sector mass spectrometer equipped with a SEM ion counting detection system (*8*).

Thorium was purified using an HCl anion column for Th−U separation and a nitric acid anion column for major element separation (*7*). Thorium was analyzed using the Isoprobe-P MC-ICPMS with multistatic collection of ^{232}Th and ^{229}Th on Faraday cups and ^{229}Th and ^{230}Th on a Daly detector. Samples were bracketed with gravimetric thorium standard solutions of known ^{232}Th/^{229}Th ratio to correct for instrumental mass fractionation and calibrate the gains between Daly and Faraday detectors.

Plutonium was purified using coprecipitations followed by anion exchange columns. The purified plutonium was then loaded onto a single resin bead that was placed in a single Re canoe carburized filament. Plutonium isotopes were measured dynamically on a GV Sector 54 mass spectrometer equipped with a Daly ion counting detector.

Measurement accuracy for both U concentration and ^{234}U/^{238}U ratio was verified by measurement of NBS U-960 and NIST 4321C natural uranium standard reference materials. For uranium and radium, filtration and process blanks are negligible in comparison to sample size. A ^{232}Th blank correction of ~43 pg was applied to the data, corresponding to < one-third of the ^{232}Th signals measured. For ^{239}Pu, an isobaric interference corresponding to the equivalent of 35 atoms ^{239}Pu/g sample was subtracted from the data and is similar in size to the total ^{239}Pu signal for each sample. Hence, no ^{239}Pu was detected in the samples, with an upper limit of ~50 atoms ^{239}Pu/g sample.

Results and Discussion

Long-lived uranium-series results (^{238}U, ^{234}U, ^{230}Th, ^{226}Ra) for samples collected in 2000−2001 are shown in Table 1. Uranium concentrations and ^{234}U/^{238}U ratios for SZ and UZ samples collected in 2003−2006 are given in Tables S1 and S2 in the Supporting Information. Uranium concentrations and ^{234}U/^{238}U ratios for unfiltered, filtered, and ultrafiltered samples are given in Table S3.

Uranium Constraints on Groundwater Flow in the Saturated Zone. In 2003, three groundwater wells were drilled directly adjacent to (PB1) and ~50 m on either side of the

TABLE 1. U−Th−Ra Disequilibria Systematics for Unsaturated and Saturated Zone Water Samples Collected in 2000−2001 Measured by Isotope Dilution Mass Spectrometry[a]

location	sample ID	date collected	[U] (ng/g)	$^{234}U/^{238}U$ (activity ratio)	[Th] (pg/g)	$[^{230}Th]$ (fg/g)	$^{230}Th/^{234}U$ (activity ratio)	$[^{226}Ra]$ (fg/g)	$^{226}Ra/^{230}Th$ (activity ratio)	$^{226}Ra/^{238}U$ (activity ratio)
unsaturated zone										
perched water from borehole at +10 level	AS-5	25-Feb-00	5.734 ± 0.011	2.856 ± 0.003	136.7 ± 0.4	3.11 ± 0.03	0.0116 ± 0.0001			
perched water from borehole at +10 level	030701-01	7-Mar-01	10.40 ± 0.02	2.051 ± 0.002				0.022 ± 0.001		0.0062 ± 0.0002
front of adit near UACH 1	030701-05	7-Mar-01	13.01 ± 0.03	1.023 ± 0.002	17.13 ± 0.13	76.1 ± 0.2	0.349 ± 0.002	54.3 ± 0.3	34.4 ± 0.2	12.4 ± 0.1
front of adit near UACH 3	AS-1	25-Feb-00	68.46 ± 0.13	1.060 ± 0.001	8.76 ± 0.06	87.7 ± 0.5	0.0737 ± 0.0005	194 ± 5	106 ± 2	8.38 ± 0.19
front of adit near UACH 5	AS-2	25-Feb-00	36.92 ± 0.07	0.939 ± 0.002	6.72 ± 0.04	5.29 ± 0.03	0.00930 ± 0.00006	202 ± 1	1840 ± 10	16.2 ± 0.1
front of adit near UACH 5	030701-04	7-Mar-01	16.49 ± 0.05	0.920 ± 0.004	0.725 ± 0.003	42.8 ± 0.1	0.172 ± 0.001	>20	>20	>3
middle of adit near UACH 7	AS-3	25-Feb-00	4.035 ± 0.008	1.177 ± 0.002	0.73 ± 0.07	0.59 ± 0.02	0.0075 ± 0.0003	76 ± 6	6200 ± 600	56 ± 4
middle of adit near UACH 7	030701-03	7-Mar-01	26.96 ± 0.05	1.173 ± 0.001	0.66 ± 0.03	2.23 ± 0.01	0.00429 ± 0.00003	>470	>10000	>50
back of adit near UACH 9	AS-4	25-Feb-00	2.872 ± 0.009	2.207 ± 0.006	1.47 ± 0.03	1.57 ± 0.01	0.0151 ± 0.0001	5.51 ± 0.04	169 ± 2	5.68 ± 0.05
back of adit near UACH 9	030701-02	7-Mar-01	1.201 ± 0.003	2.588 ± 0.005	19.0 ± 0.5	18.8 ± 0.2	0.370 ± 0.003	46.0 ± 0.6	117 ± 2	113 ± 2
saturated zone										
PB4	AS-6	25-Feb-00	2.528 ± 0.006	1.183 ± 0.003	604 ± 2	19.7 ± 0.1	0.402 ± 0.003			
Pozos Ranch	030701-06	7-Mar-01	5.711 ± 0.011	2.035 ± 0.002	<0.07			0.124 ± 0.003		0.0641 ± 0.0014

[a] Errors are 2σ. Half-lives used are 4.468×10^9 y for ^{238}U, 245,250 y for ^{234}U, 75,690 y for ^{230}Th, and 1600 y for ^{226}Ra.

FIGURE 3. Time-series of uranium concentrations in saturated zone groundwater samples near Peña Blanca. Uranium concentrations in wells drilled in 2003 (PB1, PB2, PB3) have generally exponentially decreased over time, although well pumping and conditioning in December 2003 and August 2006 disturbed the trend. Results for PB4, Peña Blanca Ranch, and Pozos Ranch have remained low over this time period. Results for December 2006 are from M. Rearick (LANL, personal communication).

Nopal I uranium deposit (PB2 and PB3). After drilling, U concentrations were elevated in all three wells (0.1−18 mg U/kg) due to drilling activities. pH values were as high as 11.3 from detergents in the drilling fluids, and interaction of these high pH fluids with surrounding rock led to the high U concentrations. pH decreased in a matter of a few months (by July 2003) to more typical groundwater values (pH = 7−9). Well productivity and SZ permeability obtained from pump tests (*9*) decreases in the order PB3 > PB1 > PB2, and this correlates with initial U concentrations. This suggests that wells with higher permeability had greater water−rock interaction. PB1 and PB2 wells were characterized by very low productivities and permeabilities (*9*). As shown in Figure 3, U concentrations for the new wells have exponentially decreased over time, although well pumping and conditioning in December 2003 and August 2006 disturbed this general trend.

Uranium isotopic and concentration data for the SZ are shown in Figure 4, in which conservative mixing between components results in linear trends. $^{234}U/^{238}U$ activity ratios are similar for PB1−PB2 (1.005−1.090) but higher for PB3 (1.36−1.97) over the 2003−2006 time period. These data, along with results of pumping (*9*) which found drawdown of PB1 during PB2 pumping and vice versa, suggest interconnectivity between the PB1−PB2 wells. However, PB1−PB2 water is distinct from PB3 in both [U] and $^{234}U/^{238}U$. Regional groundwater wells located several km from the deposit also have distinct U isotopic characteristics, indicative of multiple components of uranium. Results for 11 water samples collected from the Chuviscar River, located near Aldama, ~50 km south of the Nopal I mine, are also given in Figure 4 with $^{234}U/^{238}U$ activity ratios = 4.3 ± 0.2 (1σ; (*10*)). The river drains alluvial fans and volcanic rocks of Sierra la Gloria which are similar to those in the Peña Blanca uranium district. Multiple components shown in Figure 4 consist of (1) a high U component with $^{234}U/^{238}U$ activity ratios near unity, as would result from bulk dissolution of a rock in secular equilibrium, (2) a high U, high $^{234}U/^{238}U$ component, which reflects a greater recoil-related $^{234}U/^{238}U$ signature, and (3) a component with $^{234}U/^{238}U$ activity ratio near unity and low U concentration. Varying uranium concentrations of the components may be generated by any number of processes

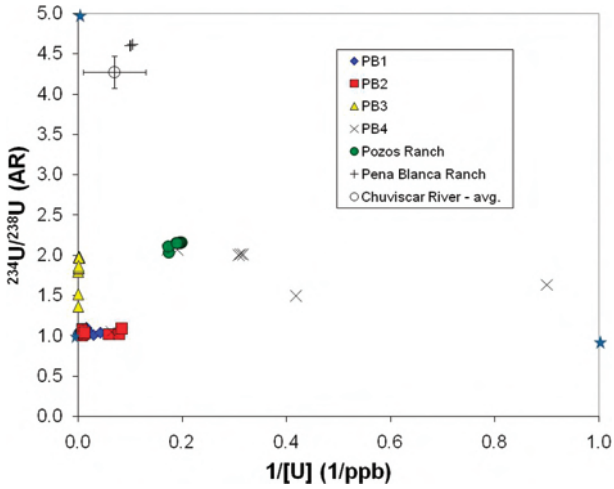

FIGURE 4. Uranium isotope mixing diagram for groundwater samples from the saturated zone. Data with 1/[U] > 1 not shown. At least three components for uranium (denoted by stars) with limited mixing among these components are indicated. An exception to this is the results for PB1 and PB2, which, along with well pumping and conditioning results, suggest interconnectivity between the groundwater in these two wells. See text for further discussion.

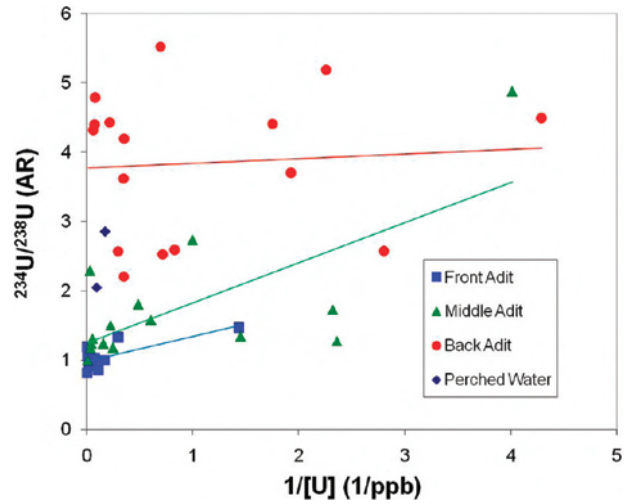

FIGURE 5. Uranium isotope mixing diagram for the adit water samples from the unsaturated zone. Data are from this study and Pickett and Murphy (*13*). Data with 1/[U] > 5 not shown. A spatial dependence for the uranium isotopic systematics is indicated, and a weak seasonal dependence may also be present (*14*). Based on a linear approximation for each region of the adit, low intercept and high slope for samples from the front and middle adit are indicative of high uranium dissolution inputs and long water−rock interaction times. Samples from the back adit have experienced lower uranium dissolution inputs and variable but generally shorter water−rock interaction times.

including dissolution/precipitation/sorption and evaporation/dilution.

Decreasing uranium concentrations in the new wells can be modeled in a variety of ways, including physical and chemical models or combinations thereof. Here we present a simple physical model that places order of magnitude constraints on groundwater flow velocity. We use a one-dimensional tank model, where the tank consists of the SZ well volume that is continuously flushed with groundwater (*11*). We assume that uranium is introduced as a slug to each of the wells and transported as a conservative tracer by groundwater flow. Hence, U concentration is a simple function of groundwater flow velocity or specific discharge. Since background U in groundwater is negligibly small compared to the U defined by the initial slug, we obtain the following relations derived for this study:

$$dC/dt = -2qhrC/V \quad (1)$$

$$q = \frac{V}{2hr(t_2 - t_1)} \ln\left(C_1/C_2\right) \quad (2)$$

where q is the groundwater specific discharge, V is the saturated zone well volume (163−208 L), h is the casing perforation height (9.15−12.20 m), C_1 is the U concentration at time t_1 and C_2 is that at t_2, and r is the well casing internal radius (4.825 cm). The model is only approximate, and additional factors are often included to account for flow distortion or skin effects from drilling, which can modify flow through the borehole relative to the surrounding formation (e.g., (*11*)). Consideration of the most likely chemical effect (U precipitation) would decrease the flow required to decrease U concentrations with time, hence the physical model above may provide an upper limit on groundwater flow rates.

The most reliable velocity data are likely obtained from the initial decrease in U concentration in 2003, when the model is relatively unaffected by the background U in groundwater. Using 2003 data for all three wells, the model yields specific discharge of 0.7−2.3 m/y. Using porosity measurements for the Pozos conglomerate of $n \approx 15\%$ (*6*), this corresponds to groundwater flow velocities ranging from $v = 5$ to 15 m/y, where $v = q/n$, and n = porosity. The slow flow velocities obtained are consistent with interconnectivity between PB1−PB2 observed during field tests (*9*), as much larger flow rates would be expected during active pumping. ^{222}Rn measurements taken before and after pumping PB1 in August 2006 also indicate a relatively low specific discharge of ~2 m/y (*12*). Consequently, the uranium concentration and isotopic results, low well productivities, and ^{222}Rn constraints suggest slow saturated zone groundwater flow with little or no regional scale mixing at this location.

Uranium Constraints on Dissolution Inputs and Residence Times in the Unsaturated Zone. Uranium isotopic systematics for all adit waters collected from 1995 to 2006, including results obtained independently by *13* are shown in Figure 5 and appear to show a spatial dependence. In general, the overall range of ^{234}U/^{238}U activity ratios for the UZ (1−6) and SZ (1−5) are similar (Figures 4 and 5). The front adit generally has ^{234}U/^{238}U activity ratios near unity and higher U concentrations, as would result from dissolution of a rock in secular equilibrium. The back adit is characterized by high ^{234}U/^{238}U activity ratios from 2 to 5 and variable U concentration, indicating a high recoil-related component and U concentration affected by varying U dissolution fluxes and/or water−rock interaction times. Finally, the middle adit appears to be a mixture of these two endmembers. There may also be a seasonal dependence, with samples collected in the wet monsoon season (July−December) tending to have higher ^{234}U/^{238}U and greater recoil signature than those collected in the January−June dry season (*14*). Here we discuss the stronger spatial dependence only.

These results can be evaluated using a model simulating a nonsteady state situation for uranium isotope transport in groundwater, which provides constraints on in situ radioisotope migration in dissolved and colloidal phases in terms of retardation factor and water−rock interaction time (*2, 14*). For uranium, the model is based on the fact that water passing through the UZ has its U concentration and ^{234}U/^{238}U ratio modified by U dissolution from rocks and α-recoil input of ^{234}U from rock surfaces. The model predicts that intermittent

UZ flushing gives rise to waters having a linear relationship between 1/[U] and $^{234}U/^{238}U$ (Figure 5).

The isotope mixing relations seen in Figure 5 appear scattered, and a linear model can only approximate the results. Similar range and scatter for the U isotopic systematics of UZ water near Yucca Mtn., Nevada was observed by (*15*). Scatter in both of these studies may be due to imperfect or insufficient sampling of the full range of natural conditions. However, the intercept and slope of the linear approximation reveals consistent results in terms of uranium dissolution inputs and/or water−rock interaction times. Samples from the front and middle adit correspond to low intercept (near secular equilibrium), reflecting increased U dissolution inputs toward the front adit, where the ore deposit is located. Their generally high U concentration and slope reflect longer water−rock interaction times. High intercept, low slope, and generally lower U concentration for samples from the back adit suggest that these samples have experienced decreased U dissolution inputs and variable but generally shorter water−rock interaction times. More detailed modeling of these results is presented in *14*.

Consistent with these results, shorter seepage times have been observed for the back adit relative to the front, based on rainfall measurements along with seepage results from transducer-monitored adit collector columns (P. Dobson, personal communication). Measured matrix permeabilities of the Nopal tuff are low (<0.1 millidarcy), thus flow through the altered tuff is predominantly controlled by fracture flow (*6*). Although there are fractures throughout the adit, the back adit is characterized by greater and more rapid fracture flow than the front adit where the deposit is located. Evaporation during rapid fracture flow in the back adit in the summer monsoon season is expected to be quite limited. However, considerable evaporation can take place during the longer seepage times at the front, and seepage from the front adit generally has higher salinity and lower volume (P. Dobson, personal communication). Similar hydrogen and oxygen isotopic compositions of seepage water from the back adit and summer rainfall, and heavier hydrogen and oxygen compositions for seepage water from the front adit (P. Dobson, personal communication) also support these conclusions.

Our preliminary results suggest that uranium dissolution inputs for the back adit for fractures with water−rock interaction times of ~0.5 days are ~1 ppb dissolved U/day. It may also be possible to determine dissolution fluxes for a wide range of elements in the UZ in the back adit, where complicating effects of evaporation and mineral precipitation on seepage water elemental abundance are relatively minor. Although we are aware of no other field measurements of this type, the U dissolution rate above can be compared to laboratory experiments which indicate rapid initial dissolution (~200−4000 ppb dissolved U/day) of soluble uranyl phases present in the suspended sediment of the Upper Puerco River, New Mexico (*16*). Our estimate is 2−3 orders of magnitude lower, presumably due to differences in water/rock ratio and uranium characteristics of solid phases.

Uranium-Series Constraints on Radionuclide Mobility. Our $^{238}U-^{234}U-^{230}Th-^{226}Ra$ disequilibria measurements for groundwater samples located primarily in the UZ (Table 1) indicate that $^{230}Th/^{238}U$ activity ratios range from 0.005 to 0.48, and $^{226}Ra/^{238}U$ activity ratios range from 0.006 to 113. Following eqs 7−9 or also 4,10 in ref *1*, for groundwater in contact with a solid matrix in secular equilibrium, activity ratios of long-lived U-series nuclides are inversely related to relative retardation factors. The rocks and uranium ores at Peña Blanca have ages greater than one million years (*4, 6, 17*), and should be near secular U-series equilibrium. In addition, younger secondary minerals deposited in fractures are also near secular equilibrium, with activity ratios ranging from

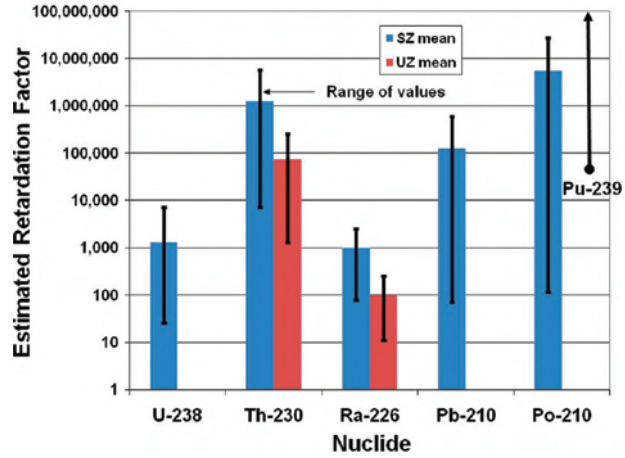

FIGURE 6. Graphical representation of the average and range of estimated retardation factors determined from U-series disequilibria for various U-series nuclides in the SZ and UZ. Average values of SZ retardation factors range from 10^3 to 10^7, and decrease in the order $^{239}Pu \approx {}^{210}Po \approx {}^{230}Th > {}^{210}Pb > {}^{238}U \approx {}^{226}Ra$. Both ^{230}Th and ^{226}Ra appear to have greater mobility in the UZ than the SZ. Results are from this study and Luo et al. (*12*).

0.9 to 1.5 for $^{234}U/^{238}U$, 1.0 to 1.5 for $^{230}Th/^{238}U$, and 0.7 to 1.2 for $^{226}Ra/^{230}Th$ (*18*). Consequently, $R_f(^{230}Th)/R_f(^{238}U)$ ranges from ~2 to 200, and $R_f(^{226}Ra)/R_f(^{238}U)$ ranges from ~0.009 to 170, where R_f is the retardation factor. Because $^{226}Ra/^{238}U$ ratios are highest in the UZ and lowest in the SZ, radium appears to have enhanced mobility in UZ waters near the deposit. This observation is similar to results obtained from U-series studies of surface fractures near the deposit, which indicate relatively recent mobility for ^{226}Ra (*18*). It is also similar to results obtained for vegetation near the deposit (*19*), which also shows high levels of ^{226}Ra relative to ^{230}Th and ^{238}U. In the absence of significant Ra/U fractionation upon plant uptake, this would also indicate greater mobility of Ra in the UZ.

We also have studied the $^{238}U-^{239}Pu$ disequilibrium systematics for four SZ groundwater samples (PB1, PB2, PB3, and PB4) collected in December 2003. We did not measure any ^{239}Pu in any of the filtered samples, with the corresponding upper limit $^{239}Pu < 50$ atoms/g (see above). Uranium systematics for samples collected at this time are quite reproducible (Table S1), with sample PB3 having the highest U concentration of 966 ppb. Assuming that the Pu in sample PB3 would be naturally derived from neutron reactions with ^{238}U, comparison of the measured upper limit Pu/U ratio (2×10^{-14}; based on $^{239}Pu < 50$ atoms/g and U = 966 ppb) with the secular equilibrium ratio (based on the average Pu/U in old uranium ores of $\sim 2 \times 10^{-11}$ (*20*)) provides constraints on the relative mobility of Pu and U in the SZ. These results indicate that Pu mobility in the SZ at Peña Blanca is at least 3 orders of magnitude lower than the U mobility. Hence, $R_f(^{239}Pu)/R_f(^{238}U)$ is calculated to be ≥1000.

By combining long-lived nuclide data from this study with short-lived nuclide data (*12*), we estimate that $R_f(^{238}U)$ varies from ~30 to 7200, with an average value of 1300 (Table S4; Figure 6). Estimates of $R_f(^{238}U)$ are obtained from eqs 5 and 9 in ref *2*, which in general at Peña Blanca reduce to $R_f(^{238}U) \approx A(^{222}Rn)/A(^{238}U)$, where A denotes activity. Estimated retardation factors for short-lived U-series nuclides are also obtained by comparing their activities with the ^{222}Rn activities, indicative of the supply rate of short-lived nuclides in the ^{238}U decay series due to recoil related effects (*1*). In addition, some samples in the UZ have values of $R_f(^{226}Ra)/R_f(^{238}U)$ near 0.01, indicating that for these samples $R_f(^{238}U) \geq 100$, since $R_f(^{226}Ra)$ must be ≥1.

Ranges of retardation factors for the SZ are ~10 to 10,000 for ^{238}U and ^{226}Ra, ~1000 to 10,000,000 for ^{230}Th, and >34,000 for ^{239}Pu. However, using the average value of 1300 for $R_f(^{238}U)$ in the SZ, the retardation factor for ^{239}Pu in the SZ is likely to be >1,000,000. On the basis of data in Table S4 and Figure 6, average values of SZ retardation factors range from 10^3 to 10^7, and decrease in the order $^{239}Pu \approx {}^{210}Po \approx {}^{230}Th > {}^{210}Pb > {}^{238}U \approx {}^{226}Ra$.

Using the average value of 1300 for $R_f(^{238}U)$ in the SZ, absolute retardation factors for U-series daughter nuclides in the UZ range from ~10 to 230 for ^{226}Ra and from ~1300 to 260,000 for ^{230}Th based on samples from the mine adit. Both ^{226}Ra and ^{230}Th have greater mobility in the UZ near the ore deposit than the SZ. Greater UZ mobility for these nuclides is an unusual characteristic which may be related to higher sulfate concentrations for the UZ and near-field SZ relative to the far-field SZ (*21*). Greater mobility does not persist into the SZ, where retardation factors return to high values more typical of groundwater systems in general (e.g., *1*−*3*).

Our results on U-series nuclide mobility at Peña Blanca can be compared to sorption data for Yucca Mountain tuff obtained from laboratory experiments (*22*). In general, K_d values for $U = 2-20$ mL/g, for Ra and Th $= 100-10{,}000$ mL/g, and for Pu $= 10-10{,}000$ mL/g. Based on the porosity and bulk density of the Yucca Mountain tuffs, retardation factors are a factor of ~10 larger than the K_d values. Results presented here are consistent with some of these trends, but not all of them. Most notably, Yucca Mountain sorption data indicate that Ra should be retarded much more strongly than U. Since Ra mobility in the SZ at Peña Blanca is typical of groundwater in general, the major difference in the data sets for the SZ appears to be related to U mobility. Namely, U mobility appears to be a factor of 10−100 higher in the sorption data set relative to in situ U-series measurements performed at Peña Blanca and other sites (*2*).

To define the uranium colloidal contribution, two SZ samples (PB1 and PB4) have been ultrafiltered in the laboratory. Uranium concentration measurements (Table S3) indicate that ~93−97% of uranium present is truly dissolved. Similar $^{234}U/^{238}U$ for unfiltered, filtered (<200-nm), and ultrafiltered (<20-nm) aliquots also support this conclusion. These results are similar to prior studies for other uranium deposits such as Koongarra (*23*), which indicate ~3% of uranium occurs as colloids. These results also agree with results for groundwater from the Nevada Test Site (*24*). However, the small fraction of colloidal uranium could have environmental implications in some cases, as it can migrate in subsurface media much faster and can travel distances much larger than dissolved uranium (e.g., (*25*)). This may be due to the presence of small quantities of highly mobile colloids in the colloid population (*26*).

To summarize, our U-series results provide initial field data on uranium dissolution inputs (~1 ppb dissolved U/day) in the UZ. At Peña Blanca, our U concentration data suggest that SZ groundwater flow rates are slow (~10 m/y). We also obtained initial constraints on $^{238}U-^{239}Pu$ disequilibrium in the SZ, with Pu mobility >1000 times lower than the U mobility. Radionuclide transport rates in the SZ are, on average, factors of 10^3 to 10^7 lower than the groundwater flow rate and decrease in the order $^{226}Ra \approx {}^{238}U > {}^{239}Pu \approx {}^{230}Th$. Both Ra and Th appear to have on average greater mobility ($\approx \times 10$) in the UZ than the SZ.

Acknowledgments

We thank Ignacio Reyes and Rodrigo de la Garza (Universidad Autónoma de Chihuahua), Alfredo Rodríguez (WWF), Paul Cook and Teamrat Ghezzehei (LBNL), and Paul Reimus, John Dinsmoor, and Ron Oliver (LANL) for valuable discussions and assistance in the field. We also thank Ardyth Simmons and Schon Levy (LANL) for project guidance. Finally, we thank the anonymous ES&T reviewers for helpful comments. This work was supported by the U.S. DOE, Office of Civilian Radioactive Waste Management (OCRWM), under contract DE-AC02-05CH11231. The views expressed in this article are those of the authors and do not necessarily reflect the views or policies of the United States Department of Energy or OCRWM.

Supporting Information Available

Table S1: Groundwater well uranium concentrations and $^{234}U/^{238}U$ activity ratios for samples collected in 2003−2006 measured by isotope dilution mass spectrometry. Table S2: Uranium concentrations and $^{234}U/^{238}U$ activity ratios for unsaturated zone samples collected from the mine adit in 2003−2006 measured by isotope dilution mass spectrometry. Table S3: Comparison of uranium concentrations and $^{234}U/^{238}U$ ratios for unfiltered samples, samples filtered in the field, and ultrafiltered samples. Table S4: Estimated retardation factors for various U-series nuclides for saturated and unsaturated zone samples. This material is available free of charge via the Internet at http://pubs.acs.org.

Literature Cited

(1) Krishnaswami, S.; Graustein, W. C.; Turekian, K. K.; Dowd, J. F. Radium, thorium and radioactive lead isotopes in groundwaters: application to the in situ determination of adsorption-desorption rate constants and retardation factors. *Water Resour. Res.* **1982**, *6*, 1663–1675.

(2) Luo, S.; Ku, T. L.; Roback, R.; Murrell, M.; McLing, T. L. In-situ radionuclide transport and preferential groundwater flows at INEEL (Idaho): Decay-series disequilibrium studies. *Geochim. Cosmochim. Acta* **2000**, *64*, 867–881.

(3) Porcelli, D.; Swarzenski, P. W. The behavior of U- and Th-series nuclides in groundwater. *Rev. Mineral. Geochem.* **2003**, *52*, 317–361.

(4) Pearcy, E. C.; Prikryl, J. D.; Murphy, W. M.; Leslie, B. W. Alteration of uraninite from the Nopal I deposit, Peña Blanca district, Chihuahua, Mexico, compared to degradation of spent nuclear fuel in the proposed US high-level nuclear waste repository at Yucca Mountain, Nevada. *Appl. Geochem.* **1994**, *9*, 713–732.

(5) Wronkiewicz, D. J.; Bates, J. K.; Wolf, S. F.; Buck, E. C. Ten-year results from unsaturated drip tests with UO_2 at 90°C: Implications for the corrosion of spent nuclear fuel. *J. Nucl. Mater.* **1996**, *238*, 78–95.

(6) Dobson, P. F.; Fayek, M.; Goodell, P. C.; Ghezzehei, T. A.; Melchor, F.; Murrell, M. T.; Oliver, R.; Reyes-Cortés, I. A.; de la Garza, R.; Simmons, A. Stratigraphy of the PB-1 well, Nopal I uranium deposit, Sierra Peña Blanca, Chihuahua, Mexico. *Int. Geol. Rev.* **2008**, *50*, 959–974.

(7) Goldstein, S. J.; Murrell, M. T.; Janecky, D. R. Th and U isotopic systematic of basalts from the Juan de Fuca and Gorda ridges by mass spectrometry. *Earth Planet. Sci. Lett.* **1989**, *96*, 134–146.

(8) Volpe, A. M.; Olivares, J. A.; Murrell, M. T. Determination of radium isotope ratios and abundances in geologic samples by thermal ionization mass spectrometry. *Anal. Chem.* **1991**, *63*, 913–916.

(9) Oliver, R. D.; Dinsmoor, J. C.; Goldstein, S. J.; Reyes-Cortés, I. A.; de la Garza, R. Initial test well conditioning at Nopal I uranium deposit, Sierra Peña Blanca, Chihuahua, Mexico. *Geol. Soc. Am. Abstr. Progr.* **2005**, *37* (7), 197.

(10) Villalba, M. L.; Colmenero-Sujo, L. H.; Montero-Cabrera, M. E.; Manjón, G.; Chávez-Aguirre, R.; Royo-Ochoa, M.; Pinales-Munguía, A. Presence of uranium in the Río Chuvíscar, state of Chihuahua, México. *GEOS* **2005**, *25*, 363–367.

(11) Drost, W.; Klotz, D.; Koch, A.; Moser, H.; Neumaier, F.; Rauert, W. Point dilution methods of investigating ground water flow by means of radioisotopes. *Water Resour. Res.* **1968**, *4*, 125–146.

(12) Luo, S.; Ku, T.; Todd, V.; Murrell, M. T.; Dinsmoor, J. C. Increased concentrations of short-lived decay-series radionuclides in groundwaters underneath the Nopal I uranium deposit at Pena Blanca, Mexico. *Eos Trans. AGU* **2007**, *88* (23), GS22A-03.

(13) Pickett D. A.; Murphy, W. M. Unsaturated zone waters from the Nopal I natural analog, Chihuahua, Mexico - implications for radionuclide mobility at Yucca Mountain. In *Scientific Basis for Nuclear Waste Management XXII*; Wronkiewicz, D. J., Lee, J., Eds.; Materials Research Society: Warrendale, PA, 1999; pp 809−816.

(14) Ku, T. L.; Luo, S.; Goldstein, S. J.; Murrell, M. T.; Chu, W. L.; Dobson, P. F. Modeling non-steady state radioisotope transport in the vadose zone - a case study using uranium isotopes at Peña Blanca, Mexico. *Geochim. Cosmochim. Acta* **2009**, *73*, 6052–6064.
(15) Paces, J. B.; Ludwig, K. R.; Peterman, Z. E.; Neymark, L. A. $^{234}U/^{238}U$ evidence for local recharge and patterns of groundwater flow in the vicinity of Yucca Mountain, Nevada, USA. *Appl. Geochem.* **2002**, *17*, 751–779.
(16) Delemos, J. L.; Bostick, B. C.; Quicksall, A. N.; Landis, J. D.; George, C. C.; Slagowski, N. L.; Rock, T.; Brugge, D.; Lewis, J.; Durant, J. L. Rapid dissolution of soluble uranyl phases in arid, mine-impacted catchments near Church Rock, NM. *Environ. Sci. Technol.* **2008**, *42*, 3951–3957.
(17) Fayek, M.; Ren, M.; Goodell, P.; Dobson, P.; Saucedo, A.; Kelts, A.; Utsunomiya, S.; Ewing, R. C.; Riciputi, L. R.; Reyes, I. Petrogenesis and geochronology of the Nopal I uranium deposit, Mexico. In *Proceedings, 2006 International High Level Radioactive Waste Management Conference*; American Nuclear Society: Las Vegas, NV, 2006; pp 55−62.
(18) Murrell, M. T.; Goldstein, S. J.; Dixon, P. R. Uranium decay series mobility at Peña Blanca, Mexico, implications for nuclear repository stability. In *Eighth EC Natural Analogue Working Group Meeting;* von Maravic, H., Alexander, W. R., Eds.; European Commission Nuclear Science and Technology (EUR 19118), 2002; pp 339−347.
(19) Leslie, B. W.; Pickett, D. A.; Pearcy, E. C. Vegetation-derived insights on the mobilization and potential transport of radionuclides from the Nopal I natural analog site, Mexico. In *Scientific Basis for Nuclear Waste Management XXII*; Wronkiewicz, D. J., Lee, J., Eds.; Materials Research Society: Warrendale, PA, 1999; pp 833−842.
(20) Curtis, D.; Fabryka-Martin, J.; Dixon, P.; Cramer, J. Nature's uncommon elements: plutonium and technetium. *Geochim. Cosmochim. Acta* **1999**, *63*, 275–285.
(21) *Natural Analogue Synthesis Report*; Report TDR-NBS-GS-000027 REV01; Civilian Radioactive Waste Management System Management & Operating Contractor; www.lsnnet.gov.
(22) *Site-Scale Saturated Zone Transport*; Report MDL-NBS-HS-000010 REV03; Sandia National Laboratories: Albuquerque, NM, 2007; www.lsnnet.gov.
(23) Payne, T. E.; Airey, P. L. Radionuclide migration at the Koongarra uranium deposit, Northern Australia - lessons from the Alligator Rivers analogue project. *Phys. Chem. Earth* **2006**, *31*, 572–586.
(24) Abdel-Fattah, A. I.; Smith, D.; Murrell, M.; Goldstein, S.; Nunn, A.; Gritzo, R.; Martinez, B.; Reimus, P. *Colloid characterization and radionuclide associations with colloids in source-term waters at the Nevada Test Site*; Report LA-UR-05-5312; Los Alamos National Laboratory: Los Alamos, NM, 2005.
(25) Kersting, A. B.; Efurd, D. W.; Finnegan, D. L.; Rokop, D. J.; Smith, D. K.; Thompson, J. L. Migration of plutonium in groundwater at the Nevada Test Site. *Nature* **1999**, *397*, 56–59.
(26) Robinson, B. A.; Wolfsberg, A. V.; Viswanathan, H. S.; Reimus, P. W. A colloid-facilitated transport model with variable colloid transport properties. *Geophys. Res. Lett.* **2007**, *34*, L09401.

ES902689E